

---

## Ecosystem feedbacks on climate at the landscape scale

Bruce P. Hayden

*Phil. Trans. R. Soc. Lond. B* 1998 **353**, 5-18

doi: 10.1098/rstb.1998.0186

---

### Email alerting service

Receive free email alerts when new articles cite this article - sign up in the box at the top right-hand corner of the article or click [here](#)

---

To subscribe to *Phil. Trans. R. Soc. Lond. B* go to: <http://rstb.royalsocietypublishing.org/subscriptions>

---



# Ecosystem feedbacks on climate at the landscape scale

**Bruce P. Hayden**

*Department of Environmental Sciences, University of Virginia, Charlottesville, VA 22903, USA*

Vegetation controls aspects of climate at all scales. These controls operate through fluxes of mass (water vapour, particulates, trace gases, condensation nuclei, and ice nuclei) and energy (latent and sensible heat, radiative exchanges, and momentum dissipation) between the biosphere and the atmosphere. The role these fluxes play in controlling minimum and maximum temperature, temperature range, rainfall, and precipitation processes are detailed. On the hemispheric scale, the importance of evapotranspiration, vegetation surface roughness, and vegetation albedo in the current generation of atmospheric general circulation models is reviewed. Finally, I assess at the planetary scale the global climate effects of biogenic emissions that are well mixed throughout the troposphere. I show that daily maximum and minimum temperatures are, in part, controlled by the emission of non-methane hydrocarbons and transpired water vapour. In many regions, a substantial fraction of the rainfall arises from upstream evapotranspiration rather than from oceanic evaporation. Biosphere evapotranspiration, surface roughness, and albedo are key controls in the general circulation of the atmosphere: climate models that lack adequate specifications for these biosphere attributes fail. The biosphere modulates climate at all scales.

**Keywords:** vegetation, climate change, temperature maximum, temperature minimum, dew-point temperature

## 1. INTRODUCTION

To what degree is climate controlled by the biosphere? This is the central question addressed in this paper. Walter & Breckle (1985) state the modern paradigm: 'Climate is the sole primary factor which influences all others—the soil, the vegetation, and, to a lesser extent, the fauna; it is in turn affected by these factors only at the level of the microclimate.' An extensive review of the literature and original analyses of climate data are used to evaluate Walter & Breckle's notion, and to make the case for a more influential role of the biosphere in determining climate at all scales.

In 1799, Noah Webster, in a paper given before the Connecticut Academy of Arts and Sciences, stated '... it appears that the weather in modern winters in the United States is more inconstant than when the earth was covered with woods at the first settlement of Europeans in the country' (Kittredge 1948). Even a cursory examination of modern climate station data from fields and forests shows that minimum temperatures are lower in the fields and maximum temperatures higher, and thus temperature ranges greater. One has to conclude that Webster's anecdote is not without foundation. In 1802, Thomas Jefferson expressed his views on the climatic consequences of the deforestation of America, and proposed that weather records be taken at every county seat to develop the data needed to document the climatic consequences of deforestation. The idea that forests and deforestation control climates, especially rainfall, can be traced back to Christopher Columbus, as reported by his son, Ferdinand Colombo (Keen 1959). The deforestation and subsequent

desertification of the Azores and Canary Islands during the period of Portuguese colonization was the basis for Columbus's belief that, because of the presence of forests, the islands of the West Indies had ample rainfall. These old ideas were propagated by Webster and Jefferson in America, and by von Humbolt and Becquerel in Europe (see Hough 1877). In his 1849 work entitled *Ansichten der Natur*, von Humbolt wrote, 'How foolish do men appear, destroying the forest cover without regard to consequences, for thereby they rob themselves of wood and water' (Kittredge 1948). In the late nineteenth century, European and American laws protecting the forests became part of the general advancement of conservation as public policy. Things changed rapidly at the end of the first decade of the this century. Chittenden, Chief of the US Army Corps of Engineers, Moore, Chief of the Weather Bureau, and Smith, Director of the Geological Survey, independently issued reports concluding that forests were insignificant in the establishment of climate, and that man's manipulation of the forests would have little impact on climate (Kittredge 1948). Walter & Breckle (1985) restated this dogma in terms of the scale limits on the vegetation controls on climate.

The pendulum of scientific thought on ecosystem controls on climate, however, is now swinging away from the position articulated by Walter & Breckle (1985) and back towards that of Columbus five centuries earlier. Anthes (1984) noted that Dominica, which is 80% forested, receives three times more rainfall than other deforested islands of the Lesser Antilles. At the annual meeting of the British Association for the Advancement of Science on August 31, 1993, the UK National Environment

arch Council reported the headline maker, ‘the rains cause the rain, not the other way around’.

concern about a fast-approaching ice age (Schneider & Row 1976) and an equally fast global warming (Schneider 1992) broke the log-jam, and it has become respectable once again to investigate and test the idea that vegetation exerts controls on climate beyond the micro-scale. The biosphere is now thought to be an essential consideration in climate control, and models projecting future climates are not thought to work without proper specification of the biosphere. Dickinson *et al.* (1986) developed the biosphere atmosphere transfer scheme (BATS) parameterization of the biosphere for atmospheric general circulation models (GCMs) that specifically deal with evapotranspiration. Avissar (1992) listed the following vegetation characteristics as essential in mesoscale atmospheric models: surface roughness, leaf area index, vegetation height, albedo, transmissivity, emissivity and temperature. In addition, he listed the following soil properties that are also needed: bulk density, roughness, water content at saturation, soil water potential, hydraulic conductivity at saturation, and emissivity. To Avissar’s list need to add water produced by evapotranspiration, organic hydrocarbons, and biogenic condensation nuclei and ice nuclei. Given the renewed interest in and the growing literature on atmosphere–biosphere feedbacks, this issue of scale limits on these interactions needs re-examination. This paper offers new analyses and reviews of existing literature on the scientific foundations of vegetation-invariant ecosystem controls on climate.

### ATMOSPHERIC MOISTURE AND MINIMUM TEMPERATURE

Dequoy (1853) asked, ‘How do they [the forests] modify the temperature of the country?’. The basic principles of the controls on daily low temperatures have been known for some time. As early as 1865, Tyndall reported that night-time temperature minimums were under the control of atmospheric gases that absorb radiation in the infrared spectrum, especially water vapour. Tyndall concluded that if all the moisture in the air over a place were removed but for a single night, it would be replaced by the destruction of every plant which freezing temperatures could kill. Since both carbon dioxide (CO<sub>2</sub>) and ozone (O<sub>3</sub>) are well mixed in the troposphere, the diurnal and temporal variations in atmospheric emissivity, and thus nocturnal radiant energy loss and temperature, are primarily due to variations in water vapour. The greater the water content of the atmosphere, the greater the retardation of radiative cooling. Water vapour in the atmosphere, in the absence of advection of air from adjacent areas, also sets the lower limit to which temperatures can fall. This temperature is known as the dew-point temperature (T<sub>d</sub>). A plot of the average minimum temperatures and average dew-point temperatures for North America east of the one-hundredth meridian illustrates this relationship (figure 1). When, on nocturnal cooling, the dew-point temperature is reached, condensation and the release of the heat of condensation begin, and the continued temperature fall is ended until all the available water vapour in the air is converted to liquid. Running *et al.* (1987) used such a regression relationship in their

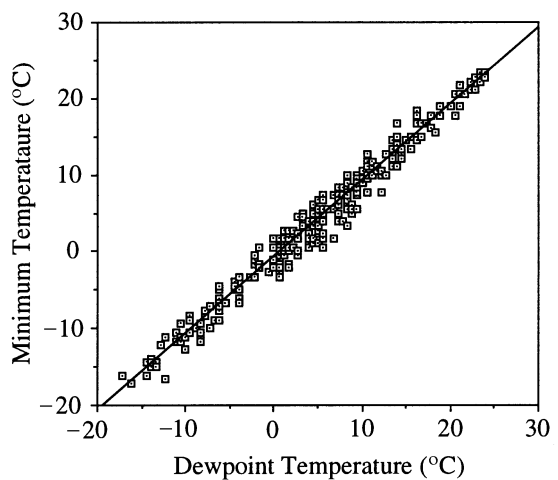


Figure 1. Average January and July mean monthly minimum temperatures and emissivity calculated from atmospheric water vapour, CO<sub>2</sub> and O<sub>3</sub> concentrations for 222 airfield weather stations in North America east of the one-hundredth meridian. The  $R^2$  for the correlation is 0.96.

MT-CLIM model to estimate dew-point temperature and, subsequently, vapour pressure deficits at midday. When atmospheric emissivity, based on the atmospheric content of water vapour, CO<sub>2</sub>, and O<sub>3</sub> (Staley & Jurica 1970), is calculated and compared with night-time minimum temperatures, a strong relationship is found (figure 2), reflecting the dominant role of water vapour in setting clear air emissivity.

Through evapotranspiration, vegetation is responsible for a portion of the total clear air emissivity. Between 10% and 55% of the water in the atmosphere over the continents comes from evapotranspiration (Rosen & Omolayo 1981; Jousaume *et al.* 1986; Brubaker *et al.* 1993). Transpired water, mixed on a daily basis through the troposphere, directly moderates temperature by increasing atmospheric emissivity and reducing outgoing terrestrial radiation, and by elevating the minimum temperature possible through dew-point temperature increases. Lettau *et al.* (1979) calculated that 88% of water vapour in the atmosphere of the upper reaches of the Amazon Basin was transpired into the air by vegetation in the basin. Lettau *et al.* (1979) found that air entering the Amazon Basin from the tropical North Atlantic typically has a water content of 18 g m<sup>-3</sup>. In spite of the substantial losses by rain during transit, by the time the air reaches the Andean foothills, the typical water content is about 25 g m<sup>-3</sup>. From Lettau’s numbers, I found that wetting of the Amazonian atmosphere corresponds to a dew-point temperature change from 21.7 °C to 26.7 °C. Even if no water was lost from the atmosphere by rain, evapotranspiration would result in minimum temperatures increasing by 5 °C. With precipitation, and without the replenishment of atmospheric moisture by evapotranspiration, 12 °C would be the average minimum temperature and, on occasion, freezing temperatures in the Amazon Basin would be possible. Evapotranspiration-enhanced dew-point temperatures are not restricted to the Amazon. Analyses of daily weather charts reveal that polar air crossing Virginia from the north-west in late April arrives at Virginia’s coast with an added amount of transpired

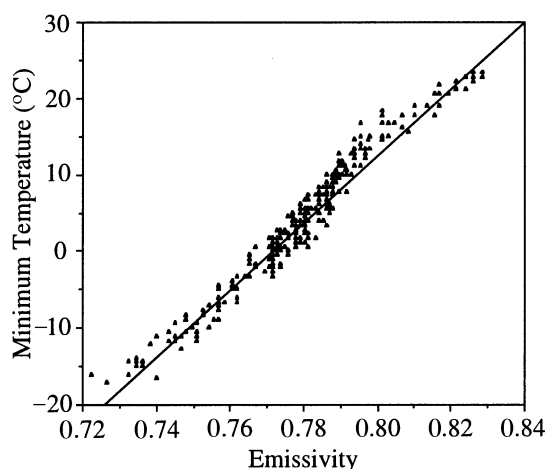


Figure 2. Average January and July mean monthly minimum and dew-point temperatures ( $^{\circ}\text{C}$ ) for 222 airfield weather stations in North America east of the one-hundredth meridian. The  $R^2$  for the correlation is 0.97.

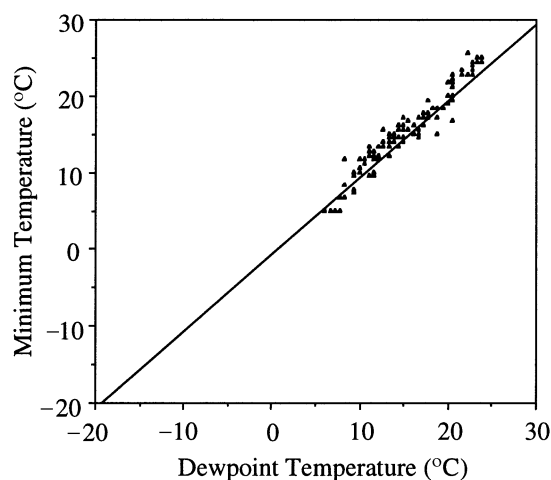


Figure 3. Average mean monthly minimum and dew-point temperatures in each month of the year for 11 airfield weather stations in vegetation-free deserts of the world. The  $R^2$  for the correlation is 0.94 ( $N=132$ ).

water vapour in the air that elevates the dew-point temperature and minimum temperatures by 4–6  $^{\circ}\text{C}$ . The minimum temperature climate of the coast of Virginia with onshore winds is moderated by the ocean, and with offshore winds the coast is moderated by the evaporation from the ‘ocean of leaves’ to the west. It is not implied here that advection of water vapour from oceanic areas is unimportant in minimum temperature controls. The analysis here does not imply that the circulation of the atmosphere that delivers this advected water vapour inland is unimportant, only that atmospheric water from terrestrial evaporation and transpiration play a significant role locally and downstream.

Figure 2 shows the relationship between calculated January and July atmospheric emissivities from  $\text{H}_2\text{O}$ ,  $\text{CO}_2$ , and  $\text{O}_3$ , and January and July monthly mean daily minimum temperatures ( $T_{\min}$ ) for 222 stations in North America east of 100 $^{\circ}$  longitude. The slope of the curve indicates that a 0.01 change in atmospheric emissivity gives rise to a 4.5  $^{\circ}\text{C}$  change in  $T_{\min}$ . Figure 1 gives the curve for  $T_{\min}$  as a function of mean daily dew-point temperature ( $T_d$ ) for the same 222 stations in eastern North America for January and July. Temperatures fall to within a degree or two of  $T_d$  during the night. This close correspondence between  $T_{\min}$  and  $T_d$  also applies to Northern Europe, South-east Asia, most of South America, polar regions, oceanic islands, and the vegetation-free deserts of the world. Figure 3 shows the relationship between monthly average, daily  $T_{\min}$  and  $T_d$  for all months of the year for 11 stations in five vegetation-free deserts. In these deserts, temperatures fall near to the dew-point temperature during the night.

Because greenhouse gases like  $\text{CO}_2$  and  $\text{O}_3$  have little geographic variation, they cannot account for the spatial variations in radiative cooling at night. Atmospheric emissivity and nocturnal cooling by radiative loss of energy vary from place to place in proportion to the water-vapour content of the atmosphere. Figure 4 shows the geographic variation in average January clear air emissivity by the method described in Staley & Jurica (1970).

All the variation here is due to geographic variations in water vapour concentrations. Figure 4 also maps the US Department of Agriculture’s (USDA’s) winter hardiness zones, reflecting winter’s average lowest temperatures. The correspondence between these two maps for the area east of the one-hundredth meridian (figure 5) has a physical basis. Hardiness zones are based on expected annual low temperatures, which are in turn a function of radiative cooling and the moisture content of the atmosphere, i.e. atmospheric emissivity. Careful examination of figure 4 indicates that a close relationship between emissivity and winter hardiness zones applies everywhere except in the south-west, where the hardiness zones are much warmer than expected based on the atmospheric emissivity. Based on water vapour,  $\text{CO}_2$  and  $\text{O}_3$  emissivities, Tucson and Washington, DC would fall within the same hardiness zone. In fact, Tucson and central Florida are within a common hardiness zone. The deserts of the south-west US have unexpectedly high minimum temperatures. This departure will be explained in a later section of this paper.

Schwartz & Karl (1990) looked at leafing-out in the spring and the wetting of the lower atmosphere by vegetation. The  $x$ -axis in figure 6 represents the time in days before and after lilac leafing-out in the Midwest. Schwartz & Karl recorded lilac leafing-out dates in a network of phenological gardens in the Midwest and North-east (Hopp 1974). The  $y$ -axis on the left side of the graph gives the water-vapour pressure of the atmosphere. On the right side of the graph, the expected daily minimum temperatures are given based on the relationship between the atmospheric water content and minimum temperatures shown in figure 1. In the 60 days before lilac leafing-out, atmospheric water-vapour pressures changed little. In the 60 days following the average date of leafing-out, the atmosphere became progressively wetter. In the days before leafing-out, expected minimum temperatures were near the freezing point. Following leafing-out, expected minimum temperatures rose rapidly, and the prospects of frost diminished as well. In the 60 days following leafing-out, dry Canadian air masses that would have made

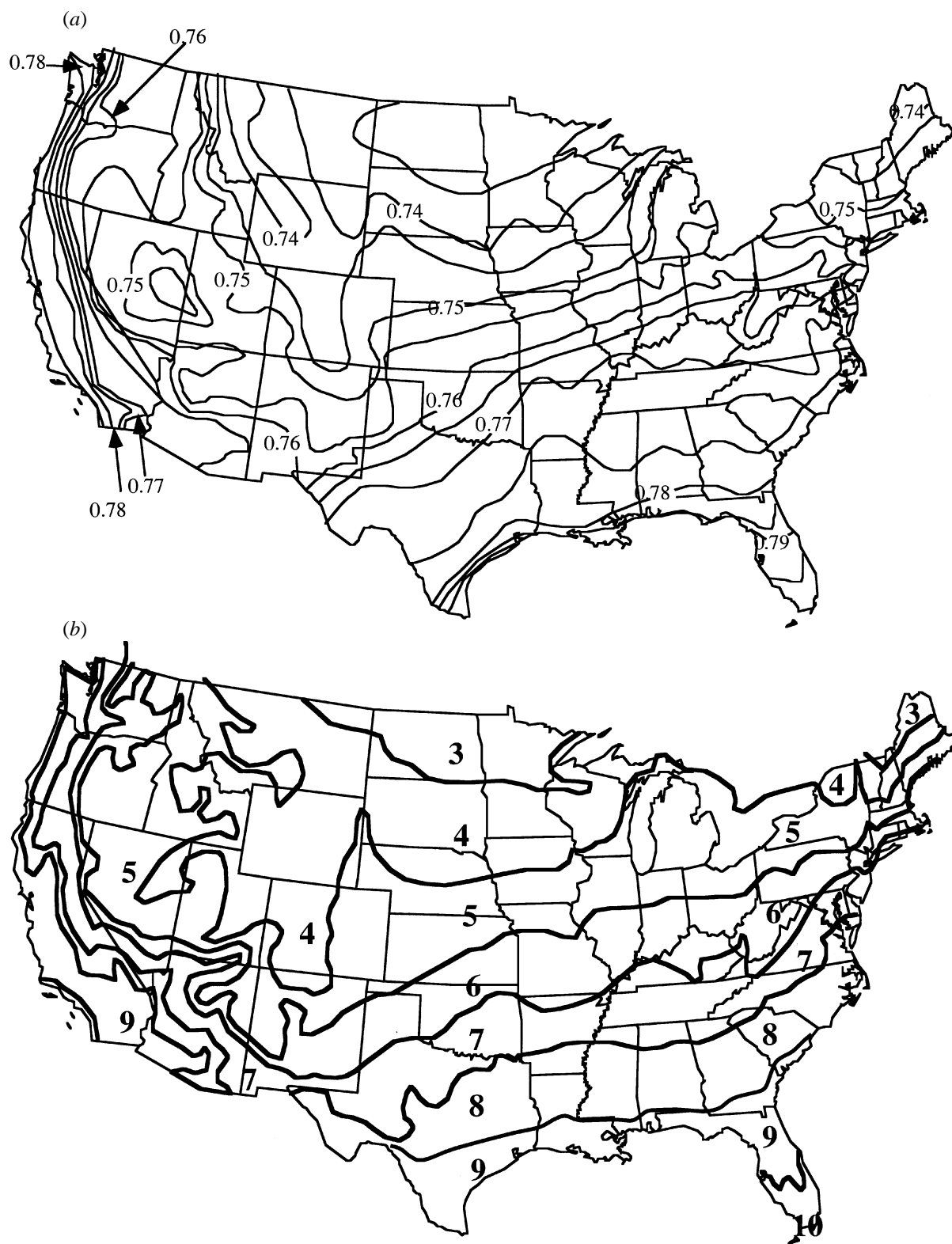


Figure 4. Clear air (cloud-free) emissivity calculated from atmospheric water vapour,  $\text{CO}_2$ , and  $\text{O}_3$  concentrations minus the emissivity overlap between water vapour and  $\text{CO}_2$ . Since  $\text{CO}_2$  concentrations are assumed to be spatially constant, the spatial variation in this clear air emissivity is that due to variations in water vapour in the atmosphere. At the bottom are the USDA's winter hardiness zones based on 1960–1990 annual minimum temperature data.

able low temperatures and frosts in the Midwest were in short supply. Frosts all the way up to 10 June are possible, but the wetting of the atmosphere by evapotranspiration greatly reduces the probability of such low temperatures. Since the leafing-out date varied widely

across the Midwest and North-east, observed increases in water vapour were probably not only from advection of wetter air over this region. Nonetheless, maritime tropical air advection into the Midwest does occur in the spring, and would elevate both dew-point and minimum

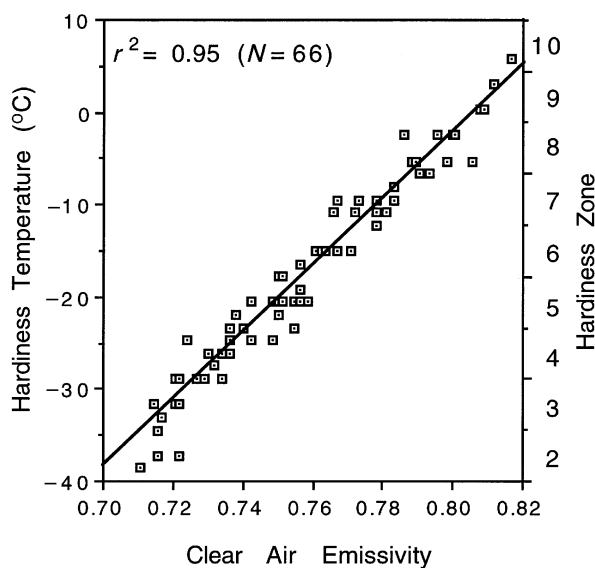


Figure 5. Eastern North American hardiness zones and hardiness temperatures as a function of clear air emissivity.

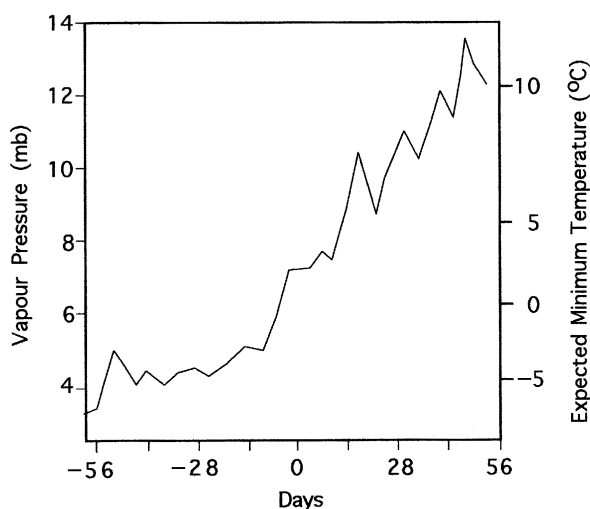


Figure 6. Atmospheric vapour pressure for 56 days before to 56 days following leafing-out, as defined by lilac plants and the expected daily minimum temperature implied by figure 1. (After Schwartz & Karl (1990), with expected minimum temperatures added.)

temperatures; but there is no reason to believe that this advection is in anyway keyed to leafing-out.

Although one might be tempted to conclude that this humidification of the atmosphere by vegetation is limited to the canopy of the vegetation, Schwartz & Karl (1990) and Schwartz (1992) reported that the increased wetting of the atmosphere is detectable up to about 3000 m during the time of leafing-out. Later in the year, as convective motions in the atmosphere begin to dominate, the moisture from evapotranspiration becomes mixed through the troposphere.

### 3. EVAPOTRANSPIRATION AND MAXIMUM TEMPERATURE

Maximum daily surface temperatures depend, in large part, on the amount of solar energy that is converted to

sensible energy at the surface. Energy flux from the surface is partitioned into latent heat and sensible heat. If water is available for evapotranspiration, up to nine times as much energy is lost from the surface by latent heating compared to sensible heating. Schwartz & Karl (1990) found that as day length and incident radiation increased during the transition from winter to spring, daily maximum surface temperatures in the Midwest increased by  $0.33\text{ }^{\circ}\text{C d}^{-1}$ . Following leafing-out in spring, the average daily increase in maximum temperatures dropped to  $0.11\text{ }^{\circ}\text{C d}^{-1}$ . The nature of heating of the lower troposphere changed with the onset of spring. Before leafing-out, the 850 mb to 750 mb layer of the lower troposphere in the Midwest warmed at a rate of  $0.11\text{ }^{\circ}\text{C d}^{-1}$ ; following leafing-out, the warming rate fell to  $0.02\text{ }^{\circ}\text{C d}^{-1}$ .

Shukla & Mintz (1982) used an atmospheric GCM to examine the effect of evapotranspiration on maximum temperatures. In the model, evapotranspiration as a source of atmospheric water was ‘turned off’. Temperatures in central North America and on other continents equilibrated at  $45\text{ }^{\circ}\text{C}$ . Using the observations of Schwartz & Karl (1990) and extending the daily (non-evapotranspiration controlled) increases in maximum temperatures of  $0.33\text{ }^{\circ}\text{C d}^{-1}$  for the 90 days from mid-April to mid-July, a warming of  $30\text{ }^{\circ}\text{C}$  would be expected. Such warming is nearly realized in desert areas where inadequate moisture is available for evapotranspiration. Recently, Fennessy *et al.* (1994) used the Center for Ocean–Land–Atmosphere (COLA) Interactions’ GCM to test the sensitivity of vegetation in thermal climates over India. When the current Indian landscape of forests and fields was replaced with a continuous broadleaf deciduous forest canopy, average June–July–August surface temperatures were reduced by  $1\text{ }^{\circ}\text{C}$ .

The evaporative flux from the biosphere depends on the available water, and thus rainfall. Figure 7 shows the relationship between annual rainfall and the average July temperature maximum for western Canada south of  $52^{\circ}\text{ N}$ . Clearly, even at these high latitudes, the case for moderation of daily high temperatures by evapotranspiration of available soil moisture is evident. Manaus, Brazil, in central Amazonia has a mean July temperature maximum temperature of  $31\text{ }^{\circ}\text{C}$ , while that of Washington, DC is  $30\text{ }^{\circ}\text{C}$ . In fact, where and when sunlight and average or greater than average rainfalls occur, these are typical maxima. From 1940–1970, the record highest July temperature in Manaus was  $35\text{ }^{\circ}\text{C}$  and  $38\text{ }^{\circ}\text{C}$  in Washington, DC. Washington is more prone to drought and periods of inadequate water resources for evapotranspiration than Manaus, and it experiences greater temperature extremes than Manaus. In contrast, arid Canyon Fields, Utah, is at the same latitude as Washington, DC, and has a July mean maximum temperature (1940–1970) of  $37\text{ }^{\circ}\text{C}$ ,  $7\text{ }^{\circ}\text{C}$  higher than that of Washington. In the Great Plains of the US, the average daily temperature in the third driest years is  $3\text{ }^{\circ}\text{C}$  higher than the mean (Borchert 1950). Chang & Wallace (1987) tabulated the 25 hottest summers in the Great Plains, and all but three were drought years. In Charlottesville, Virginia, during dry weather, temperatures frequently rise above  $33\text{ }^{\circ}\text{C}$ . In such periods, a half-inch (2.5 cm) rainfall will suppress maximum temperatures below  $32\text{ }^{\circ}\text{C}$  for about five days. If there is no additional rainfall, daily

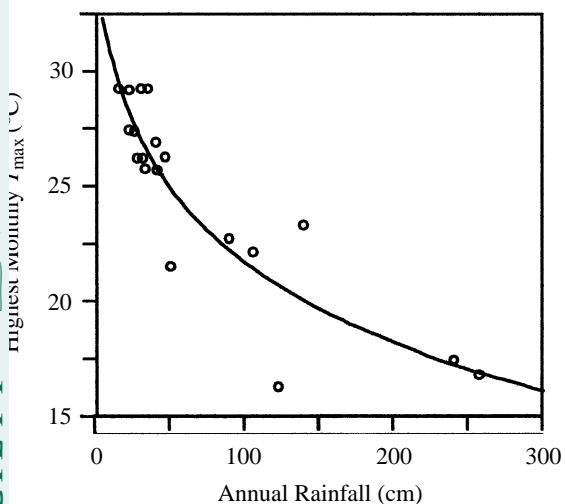


Fig. 7. Maximum monthly temperature for western Canada at 52° N and west of Winnipeg as a function of annual rainfall. The smooth curve ( $y = 105 - 20.9 \log(x)$ ) explains 90% of the variation in the data.

Maximum temperatures increase above 32 °C. Temperatures of 32 °C or less are common when cloud cover is massive and temperatures above 32 °C can occur if there is a strong advection of very warm air from distant sources. The theoretical basis for a 32 °C maximum temperature limit for well-watered vegetation is found in Monteith & Taylor (1972). They found that the rate of sensible heating goes to zero as the temperature of the atmosphere goes to 32 °C. If temperatures rise above 32 °C for other reasons, then there is a negative sensible-heat flux from the leaves from the atmosphere. Where vegetation is well-watered and wilting is not present, leaf temperatures do not exceed 32 °C.

Evapotranspiration from land surfaces loads the atmosphere with water vapour, reduces the sensible heating of the surface layer of the atmosphere, and provides a means of energy transport to higher altitudes and over greater horizontal distances. Shukla & Mintz (1982) ran the Goddard Laboratory for Atmospheric Sciences (GLAS) GCM with maximum soil moisture, and thus maximum evapotranspiration, and with a dry soil and no evapotranspiration. Without evapotranspiration loading of the atmosphere over the continents, precipitation on all continents was reduced by 50% or more. Temperatures over the continents were 25 °C hotter without evapotranspiration. Pressure fields were fundamentally altered. Tropical cyclones over subtropical oceans had 15–20 mb lower central pressure, and over land areas pressures were as much as 15 mb lower. The pattern and the strength of surface wind fields in the model were fundamentally different than in the control model run with no evapotranspiration. GCMs require adequate estimates of evapotranspiration, and this need may best be provided by ecosystem models as part of the GCM. Two types of models are currently used: BATS (Dickinson *et al.* 1986) and SiB (Sellers *et al.* 1986). BATS and SiB are simple canopy models that parameterize evapotranspiration through specifications of stomatal resistances. Future GCMs must incorporate changes in vegetation cover type and quality to adjust evapotranspiration

estimates as the model is running. As climate changes, the vegetation cover also changes and, consequently, the parameterizations for BATS or SiB require adjustment as changes within the GCM proceed. In preparation for these interactive biosphere–atmosphere models of the future, ecologists will have to develop data bases on BATS and SiB parameters for each vegetation and land-cover type at spatial resolutions of about 1° latitude by 1° longitude. These data bases will have to be at least monthly to incorporate the phenology of the biosphere (Schwartz 1998). It is likely that this temporal dynamic will require remote satellite data to obtain measures of leaf area index (LAI), soil moisture status, and vegetation status (Nemani *et al.* 1993; Running *et al.* 1994).

#### 4. BIOGENIC HYDROCARBONS AND MINIMUM TEMPERATURES

In 1865, Tyndall measured the infrared absorption of many different plant volatiles and reported absorption 30–300 times greater than that of ambient CO<sub>2</sub>. Tyndall's work on CO<sub>2</sub>, H<sub>2</sub>O, and O<sub>3</sub> absorption of terrestrial radiation led Arrhenius, in 1896, to calculate the climatic consequences of doubling atmospheric CO<sub>2</sub>. In the 1970s and 1980s, GCMs were used to estimate the consequences of doubling CO<sub>2</sub> and Arrhenius's geography of global warming was verified to a remarkable degree (Manabe & Wetherald 1975; Hansen *et al.* 1981). These models, however, do not include the radiative effects of biogenic hydrocarbons as important greenhouse gases. The planetary atmospheres specified in the GCMs are free of gaseous and particulate non-methane hydrocarbons and do not include their effects.

Non-methane hydrocarbons produced by plants include terpenes, hemiterpenes, semi-volatiles, aromatics, and cuticular waxes (Rasmussen & Went 1965; Moore 1976). Global non-methane biogenic hydrocarbon production is estimated to be from 45 to 440 × 10<sup>6</sup> t yr<sup>-1</sup> (Peterson & Junge 1971; Rasmussen 1972; Davies 1974). Roughly half the volatile biogenic hydrocarbons agglomerate as particulate hydrocarbons, and the rest remain in the vapour phase (Duce *et al.* 1974). Global hydrocarbon production is reported to be ten times greater from biogenic sources than from fossil-fuel use (Went 1960; Robinson & Robbins 1970; Peterson & Junge 1971). Terpenes usually account for about two-thirds of the hydrocarbons present over natural landscapes. Particulate hydrocarbons range in size from 0.01–0.40 μm, scatter and polarize light in the blue wavelengths, and form the well-known blue haze of vegetated regions (Tyndall 1865; Went 1960; Robinson & Robbins 1971). At relative humidities above 70%, water vapour condenses on particulate hydrocarbons (Pkhlagov *et al.* 1987); the resulting 'wet'-haze particles (haze particles enveloped in water) are 0.5–10 μm in size and scatter light at all visible wavelengths. The resulting haze is white (Went 1960; Pkhlagov *et al.* 1987). The wet-haze particulates are not as effective infrared absorbers as dry-haze particles (Pkhlagov *et al.* 1987). In the presence of NO<sub>x</sub> or O<sub>3</sub>, and light, dark-coloured smog results (Went 1960; Pkhlagov *et al.* 1987).

Atmospheric emissivity calculations used in most climate models include only absorption of terrestrial radiation by H<sub>2</sub>O, CO<sub>2</sub>, and O<sub>3</sub> as the sum of the individual

emissivities of gas minus the emissivity overlap between H<sub>2</sub>O and CO<sub>2</sub> (Staley & Jurica 1970). Methane and nitrous oxide are sometimes added to the calculation. Although molecules with carbon-carbon and carbon-hydrogen bonds are known to absorb in the infrared, the role of biogenic hydrocarbons as absorbers of terrestrial radiation has received only modest attention to date. Robinson (1950) reported that the downward flux of atmospheric radiation during hazy conditions exceeded the computed flux, and attributed the difference to 'aerosols or unspecified trace gases' (Robinson 1968). The difference between observed and calculated emissivity was greatest in dry air (Robinson 1950). Robinson found that on a day with very dry air (1 cm path length of water vapour), measured emissivity was a very large, 0.18 higher than calculated emissivity based on atmospheric H<sub>2</sub>O, CO<sub>2</sub>, and O<sub>3</sub> concentrations. For rather wet air (5 cm path length) the excess emissivity was 0.04. Robinson (1968) reported emissivities 0.09–0.18 higher than emissivities calculated for the lowest 3000 m of the atmosphere. Robinson attributed the differences to trace gases in the atmosphere during the hazy conditions of the study. In 1967, Sellers & Dryden (figure 8) found that calculated emissivities underestimated observed emissivities by 0.04–0.05 at Tucson, Arizona, when visibility was over 30 miles (Sellers & Dryden 1967). Staley & Jurica (1971) concluded that the difference between calculated and measured emissivities in the data of Sellers & Dryden should be attributed to 'as yet unidentified trace gases'. Figure 9 shows the absorption spectra for the atmosphere with specific absorption of water vapour, CO<sub>2</sub>, and O<sub>3</sub>, and a second spectral curve for absorption of a dry atmosphere with 10 ppb of alpha-pinene hydrocarbon (Stephens & Price 1970). Although absorption spectra for the diverse assemblage of hydrocarbons emitted by plants have not been determined, it is well known that carbon-carbon bonded molecules are strong absorbers of radiation at the wavelengths of terrestrial radiation. In an earlier study (Robinson 1950) where observed emissivity was significantly higher than calculated emissivity, the difference was attributed to strong absorption in the atmospheric window near 10 μm. In areas with active photosynthesis and dry air, non-methane hydrocarbons should elevate atmospheric emissivities and retard nocturnal cooling. Under such conditions, temperatures may not fall to the dew point. Figure 10 shows the relationship between dew-point temperature and average daily minimum temperatures in all months of the year for the warm, vegetated deserts of the world. With sufficient rainfall to support vegetation, temperatures in these warm deserts rarely fall to the dew point. In contrast, very low rainfall, vegetation-free deserts typically have average daily minimum temperatures close to the dew point (see figure 3). Figure 11 shows the difference between  $T_{\min}$  and  $T_d$  for the western US in January and July. In January, the desert vegetation of the Mojave, Sonoran, and Chihuahuan deserts is photosynthetically active and  $T_{\min}$  is higher than  $T_d$  by as much as 12 °C. In the summer, the vegetation is photosynthetically active everywhere in the western US and  $T_{\min}$  is significantly higher than  $T_d$  everywhere except where average daily relative humidities reach and exceed 70%. These exceptions include the Pacific North-west and alpine areas in the high altitudes of the Rockies. The

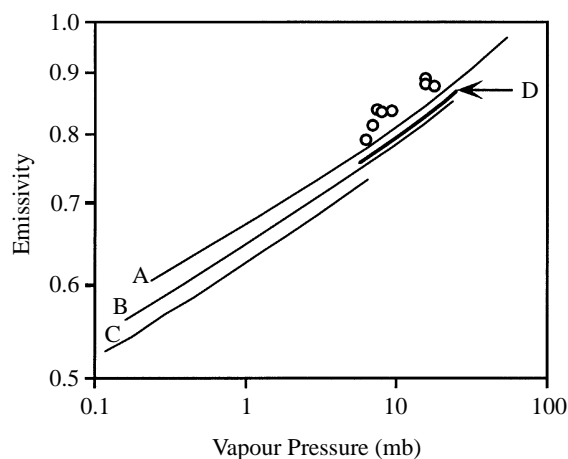


Figure 8. Calculated atmospheric emissivity for three pressure-altitude levels (A, B and C) and measured emissivity at Tucson, Arizona, indicated by the dashed line. Curve D is the expected emissivity for Tucson based on its average station pressure elevation of 910 mb. The circles represent observations of Sellers & Dryden (1967).

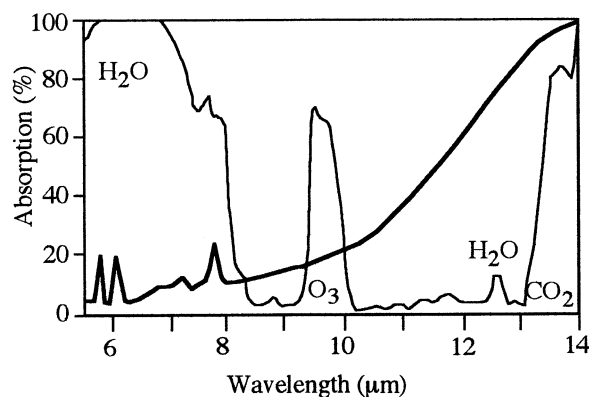


Figure 9. Atmospheric absorption by water vapour, O<sub>3</sub> and CO<sub>2</sub> (thin curve) versus absorption by 10 ppb of alpha-pinene gas in dry air (thick curve). (Data from Stephens & Price 1970).

effect is independent of latitude and, therefore, the length of the period of darkness. Figure 12 shows the difference between average monthly  $T_{\min}$  and  $T_d$  for a wide range of average monthly relative humidities for desert and non-desert areas ( $N=1008$ ). The elevation of  $T_{\min}$  above  $T_d$  is largely restricted to locations with average daily relative humidities below 70%. At high relative humidities, particulate hydrocarbons in the atmosphere become covered with water and behave radiatively as water drops, and the hydrocarbon contribution to atmospheric emissivity is minimized. This wetting and enveloping of particulate matter are functions of relative humidity not absolute humidity. Particulate matter grows in size by the condensation of water only when relative humidities exceed 70%. In regions where minimum temperatures are usually close to the dew-point temperature, relative humidity is low during the day. Figure 13 shows the difference between daily minimum and dew-point temperatures at various maximum daily relative humidities. Also shown is the accumulative frequency of days with various maximum relative humidities for Richmond, Virginia. Most days in



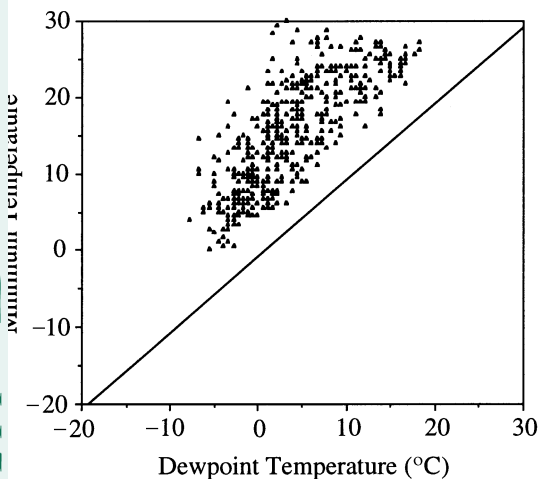


Figure 10. Monthly minimum temperatures for the warm parts of the world as a function of mean monthly dew-point temperatures (all months included). The straight line in the lower right represents the line for equal minimum and dew-point temperatures (see figure 1).

...mond reach a relative humidity of 100% in the early morning hours. On days when minimum temperatures do not fall to the dew-point temperature, atmospheric hydrocarbons may limit radiative loss of energy from the atmosphere and keep minimum temperatures above the dew-point. In mean monthly statistics, however, minimum and dew-point temperatures are essentially the same, and any greenhouse warming by non-methane hydrocarbons is swamped in climatic averaging. Warming by non-methane hydrocarbons, however, would explain elevated minimum temperatures in the warm, dry parts of the south-west US, and the unusually high-temperature zones in that region.

...the Mojave, Sonoran, Chihuahuan, and Saharan deserts are warm deserts characterized by tropical and subtropical flora and fauna, yet, if the vegetation in these deserts did not produce volatile hydrocarbons and release water vapour, they would be cold deserts with freezing temperatures in winters. Average monthly minimum temperatures in the Tarn Ghat, Libya, in a vegetated area of the northern Sahara (figure 14) are 10–35 °C higher than  $T_d$ . In un-vegetated areas, temperatures fell to the dew point in this vegetated area, all months would have freezing temperatures. In the vegetation-free deserts of Mauritania, average monthly minimum and dew-point temperatures are essentially the same. Low temperatures in arid, vegetated deserts of the world are in part controlled by desert systems.

...even the apparent magnitude of the biogenic greenhouse gas effect and the extent of arid and semi-arid lands (10% of the world's land surface), it is reasonable to propose that the next generation GCMs should include the emissivity of non-methane hydrocarbon greenhouse gases. Estimates of such emissivities may be derived from the difference between the dew-point and recorded minimum temperatures at the rate of 0.01 emissivity units for each °C in which the recorded minimum temperature exceeds the dew-point temperature. It should be noted that doubling of CO<sub>2</sub> results in a rise in emissivity of about 0.05, and an estimated 2.7 °C rise in global temperature.

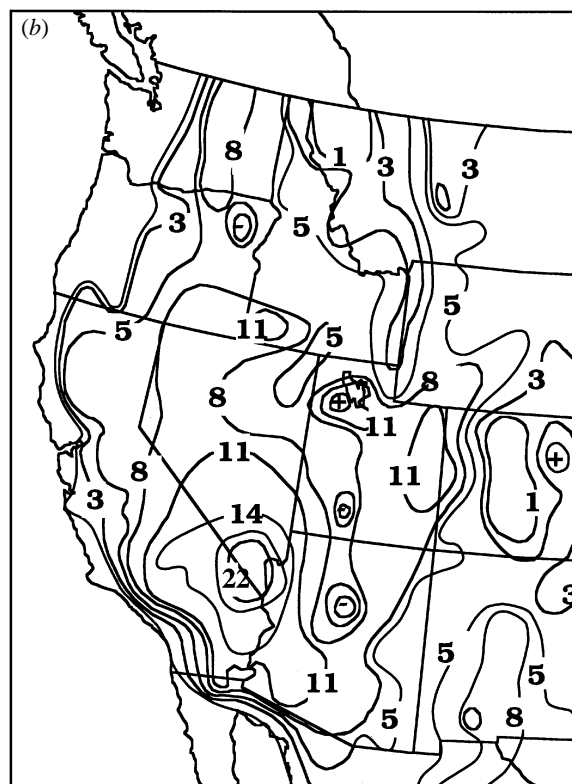
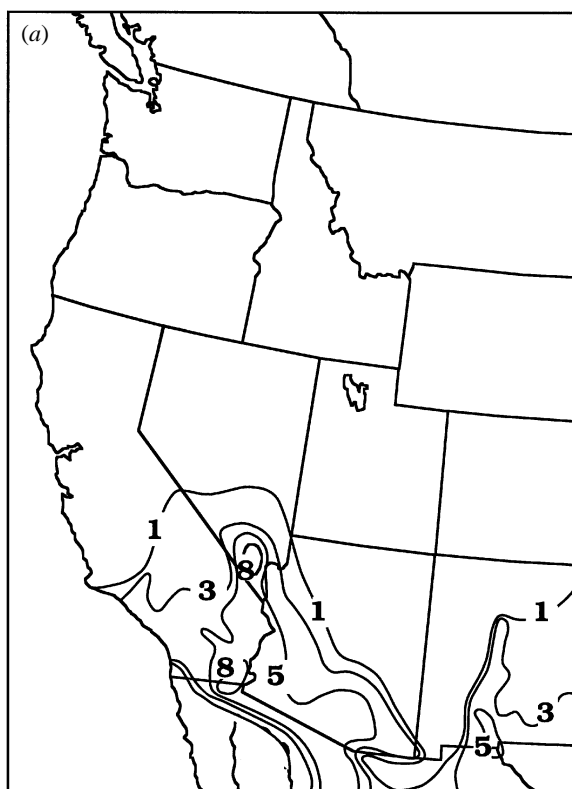


Figure 11. Mean January (a) and July (b) minimum minus dew-point temperature differences for the western United States.

GCMs with a diurnal cycle and a natural, 'dirty', Earth-like atmosphere still need to be developed. Where relative humidity is low, biogenic greenhouse gases elevate emissivities locally, and produce local greenhouse warming up to

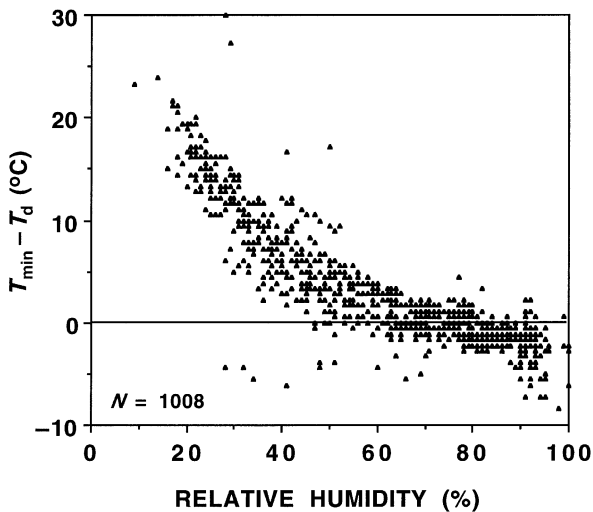


Figure 12. Monthly mean minimum minus dew-point temperature differences as a function of monthly mean relative humidity for all of North America ( $N=1008$ ).

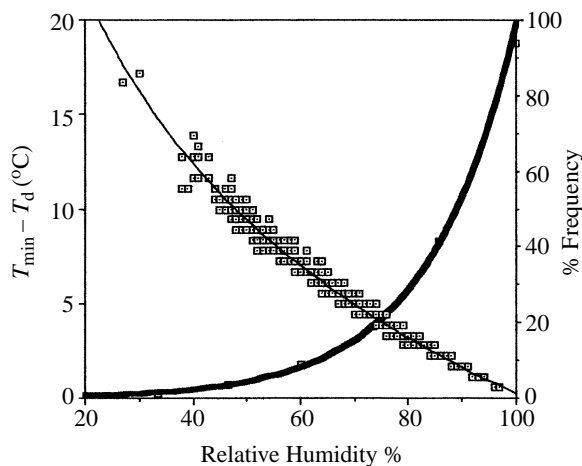


Figure 13. Average daily minimum temperature minus dew-point temperature as a function of maximum daily mean relative humidity for Richmond, Virginia (thin line). The accumulative frequency of daily maximum relative humidities at Richmond, Virginia, is shown as a bold line.

five times greater than that which would result from doubling atmospheric  $\text{CO}_2$ . Anthropogenic and natural desertification may well have important regional and global consequences as photosynthetic surface is lost and non-methane hydrocarbon production limited.

## 5. ECOSYSTEM CONTROLS ON PRECIPITATION PROCESSES

Aitken condensation nuclei are submicroscopic particles on which supersaturated water vapour condenses and forms cloud droplets. In continental regions, condensation nuclei are readily available and are of both biogenic (Woodcock & Gifford 1949; Went 1964, 1966; Went *et al.* 1967; Schaefer 1970) and anthropogenic origin (Went *et al.* 1967; Hudson 1991). The organic nature of Aitken condensation nuclei is evident in the strong diurnal and seasonal cycles in atmospheric concentrations. Numbers

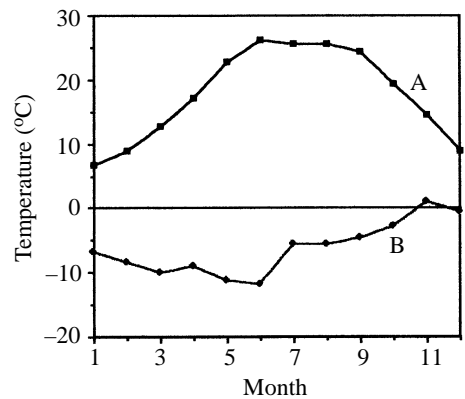


Figure 14. Mean monthly minimum temperatures (A) and mean monthly dew-point temperatures (B) for Ghat, Libya.

decline after sunset and rise sharply after sunrise. The terpenes, limonene, and alpha- and beta-pinenes, when present in the atmosphere, cause large increases in the formation of larger particles from Aitken nuclei at which point they can serve as cloud condensation nuclei (CCN) (Shaefer 1970). The size of the Aitken condensation nuclei increases throughout the morning hours as gas-to-particle conversion progresses and small nuclei grow to larger haze-size droplets. The origin of haze droplets by this gas-to-particle process in light was first demonstrated by Tyndall (1865). Haze droplets, which also arise from non-biogenic hydrocarbons and anthropogenic hydrocarbons, are excellent CCN (Junge 1951). As winds and convection increase through the morning and afternoon hours, nuclei are mixed upward through the troposphere (Went *et al.* 1967). Suitable nuclei in the lowest half-kilometre of the atmosphere are on the order of  $2.2 \times 10^{10} \text{ m}^{-3}$ . In the next half-kilometre aloft, only half as many nuclei are available, and the decline continues upward. There are ten times as many condensation nuclei over land as there are over the oceans. CCN are not limiting in cloud formation over the continents, but are limiting over the oceans. The role of the biosphere in CCN needs to be investigated as the cloud microphysical processes must be included in the next generation of GCMs. There is evidence that both cloudiness and cloud brightness depend on the number of CCN in the atmosphere (Wigley 1989; Williams *et al.* 1980).

Few CCN of continental origin are found in the marine air far from land. CCN in the marine atmosphere are sulphates that form from dimethyl sulphide (DMS) produced by marine phytoplankton (Charlson *et al.* 1987). The central idea in this hypothesis is that the oceanic cloudiness is limited by the availability of CCN, and that clouds are regulated by phytoplankton DMS production (Andreae 1980), which in turn is dependent on sea surface temperature, a variable under the control of clouds. Charlson *et al.* (1987) proposed a negative feedback on planetary thermal climate: (i) the oceans warm, by any cause; (ii) phytoplankton DMS production increases; (iii) more clouds form, planetary albedo increases, solar radiation is reduced; and (iv) cooling results. By Charlson's calculations, a 30% increase in marine CCN increases planetary albedo by 0.005 or a  $-0.7\%$  reduction in solar radiation and a planetary temperature fall of  $-1.3 \text{ K}$ .

ough the sensitivity of this negative feedback on steady temperatures is being actively debated (Wartz 1988), the role of phytoplankton as a source of material that could serve as CCN is not.

To realize rainfall from cloud drops, the drops must first increase in size. Drop sizes increase when cloud air is slightly supersaturated with water vapour. The vapour-pressure deficit of the drop relative to the surrounding air permits continued deposition of vapour on the drop. However, this process is slow and cannot account for the observed rate of raindrop growth. If temperatures are sufficiently low the cloud drops may freeze. The vapour-pressure deficit between the ice and the slightly supersaturated cloud air is large, and water vapour readily condenses on the ice and growth in ice particles is rapid. Subsequent cloud-drop growth occurs by collision of drops of unequal size. Drops of pure water of cloud-drop size will freeze spontaneously at temperatures of ca.  $-10^{\circ}\text{C}$ . Freezing at warmer temperatures requires a nucleation of the cloud drop by a substance on which ice crystallization can begin. Such impurities are known as ice nuclei. Kaolinite, a common clay mineral, causes cloud droplets to become ice at ca.  $-25^{\circ}\text{C}$ . Sea salts induce ice nucleation around the same temperature. Freezing at lower temperatures is common, and is the result of ice nuclei of biological origin. Without biogenic ice nuclei, cloud drop growth is retarded; time of rainfall may be extended and rainfall rates limited.

Most ice nuclei that exist in the atmosphere arise from the decomposition of organic matter (Vali *et al.* 1976; Spongberg & Vali 1972). Freezing temperatures in the atmosphere depend on the specific nature of the available inorganic decomposition products. Biogenic nuclei have been shown to cause freezing at temperatures as warm as  $-3^{\circ}\text{C}$ . Schnell & Vali (1973) showed that freezing temperatures of ice nuclei varied from biome to biome, with the coldest freezing-temperature ice nuclei occurring in the tropical forests and the warmest freezing-temperature ice nuclei in the high-latitude forests. The biogenic specificity remains unexplained. Some marine phytoplankton also produce ice nuclei as well (Schnell 1975; Spongberg & Vali 1976) but, generally, the marine air has few ice nuclei. Rising motions of the air within clouds are typically aided by freezing of cloud drops as growth on ice crystals is more rapid and latent heat release is greater compared to that from liquid cloud drops. Because vertical air motions and larger raindrops are required to produce cloud separation and electrical discharges, electrical storms at sea are uncommon compared to terrestrial storms. The rarity of lightning at sea is evident in both ground and direct satellite observations. The magnitude of production of ice nuclei from organic decomposition has also been shown to vary seasonally (Lander *et al.* 1975; Schnell *et al.* 1980).

When the next generation of GCMs is built, they will probably need to have higher spatial resolution ( $1^{\circ}$  latitude  $\times$   $1^{\circ}$  longitude) and include cloud microphysics. With these developments, there will be an increasing need to include condensation nuclei numbers and a biosphere-specific spectrum of ice nuclei by freezing temperatures. Further research and a global data base on ice-nuclei quantity and quality will be required. Transient GCMs with a biosphere that evolves in model time in response to

changing climate might then have an evolving spectrum of ice nuclei, and thus a feedback to the climate model.

## 6. CONTROLS ON PRECIPITATION BY TRANSPIRED WATER

Rasmusson (1967, 1968, 1971) calculated the water balance for North America and concluded that significant evaporation and evapotranspiration from the continent were required to balance his budget. Rosen & Omolayo (1981) calculated the water-vapour mass fluxes from the oceans to continents and from continents to oceans for the Northern Hemisphere. They found that, averaged over all months and all latitudes, there was a net flux from oceans to continents of  $2.73 \times 10^8 \text{ kg s}^{-1}$ ; however, in the latitude band  $30^{\circ}\text{N}$  to  $50^{\circ}\text{N}$ , there was a  $0.64 \times 10^8 \text{ kg s}^{-1}$  net flux across the coasts to the oceans. The amount of rain that is transpired to the air over the continents and returned as rain before exiting the coastal margins is not included in Rosen & Omolayo's analysis. Salati *et al.* (1979) used stable isotopes to determine the role of transpired water versus oceanic water in rainfall in the Amazon, and concluded that more than half of the water that fell was transpired water. Lettau *et al.* (1979) calculated the fraction of rainfall in the interior of Amazonia that came from evapotranspiration, and concluded that 88% of the rainfall that fell in the westernmost portion of the Amazon Basin came from transpired water. Nobre *et al.* (1991) used a GCM to study the effects of deforestation in Amazonia, and concluded that removal of the forests would reduce precipitation by 25%. Shukla & Mintz (1982) used the GLAS GCM to study the influence of evapotranspiration on subsequent precipitation, and concluded that, for eastern North America, reliance only on oceanic water resulted in rainfall reductions 3–60%. Joussaume *et al.* (1986) used a GCM to determine the origin of water in precipitation and found that, for North America east of the Rocky Mountains and north of the Gulf Coast coastal plain, over 40% of the water that fell as rain was transpired terrestrially from surfaces. Brubaker *et al.* (1993) developed a 'stream tube' to determine the role of evapotranspiration in subsequent rainfall. For the central Great Plains, evaporation and evapotranspiration from the grasslands contributed 15% to subsequent rainfall in December, up to a maximum contribution of 34% in July. In the Sahel of Africa, Brubaker *et al.* (1993) found that evapotranspiration from the Sahel accounted for as little as 10% of the rainfall in June to as much as 48% in August. The analyses by Joussaume *et al.* (1986) clearly showed that the contribution of ocean evaporation to rainfall drops to less than 50% within 700 km inland from the coast. The role of transpired water in rainfall, recycled rain, is substantial and markedly higher than the 10% or less estimated from earlier reservoir studies.

## 7. CONTROLS ON CLIMATE BY VEGETATION SURFACE ROUGHNESS

On an annual average basis, about  $3.1 \text{ W m}^{-2}$  of the  $345 \text{ W m}^{-2}$  of solar energy from the sun goes to produce kinetic energy, i.e. to generate winds (Oort 1964). The Earth as a thermodynamic system is dissipative. By

means of friction, the  $3.1 \text{ W m}^{-2}$  of energy are returned as heat and eventually released to space as terrestrial radiation. A large fraction of this energy used to make the winds blow is dissipated by the friction offered by vegetation on terrestrial surfaces and waves at sea. For example, wind speeds over the oceans adjacent to the UK average  $12 \text{ m s}^{-1}$ , while the average wind speeds over England's and Scotland's interiors are only  $6 \text{ m s}^{-1}$ . Vegetation and other roughness elements on the landscape slow the wind's speed by a half. The roughness offered by vegetation slows the winds as surely as the sun sets them in motion. To put into perspective the importance of the  $3.1 \text{ W m}^{-2}$ , consider that a doubling of atmospheric  $\text{CO}_2$  is a perturbation of only  $2.2 \text{ W m}^{-2}$ . Improper specification of the surface roughness offered by terrestrial vegetation results in large errors in GCM results (Sud & Smith 1985a,b).

Sud & Smith (1985a) investigated the role of surface roughness specification in desert areas on numerical simulations of the atmosphere using the GLAS GCM. GCMs often generate excess rainfall over observed climates in desert regions. Sud & Smith (1985b) used a sensitivity analysis to assess the role of surface roughness. The control-model run set surface roughness at 0.45 m everywhere, which was the surface roughness used in contemporary GCMs. The experiment-model run used a surface roughness of 0.0002 m for the Sahara desert and 0.45 for all other land areas. Where the desert surface roughness was properly included, Saharan rainfall was reduced over the control runs because of the new pattern of regional convergence of water vapour and rain clouds that resulted. In addition, the experiment model positioned the intertropical convergence zone to about  $14^\circ \text{ N}$ , which is closer to its normal position in July ( $10^\circ \text{ N}$ ), and thus corrected earlier versions of the model on the position of this important climatic boundary. Sud & Smith noted that lands become less rough in desertification, which further promotes desertification. Sud & Smith (1985) also looked into the sensitivity of the Indian monsoon to variations in surface roughness. They found that reducing the surface roughness from 0.45 to 0.0002 m reduced the strength of the monsoon and the rainfall rate. Most GCMs use either a constant surface roughness or drag coefficient in all terrestrial regions, or have a variable roughness at the scale of  $5^\circ$  latitude by  $5^\circ$  longitude.

Because direct measurements of surface roughness require recording a vertical profile of wind speed over the terrain of interest, direct measurements are few. In general, surface roughness is proportional (nonlinear) to vegetation height. Surface roughness is also dependent on wind speed, as vegetation becomes streamlined at higher wind speeds. In their current forms, GCMs do not generate such extreme winds. Mean wind speeds are typical model values, and singular estimates of surface roughness can be used for given land covers.

## 8. ECOSYSTEM CONTROLS ACROSS CLIMATE SCALES

Anthes (1984) considered the effects on climate of vegetation patchiness ( $10 \times 10 \text{ km}$ ) compared to bare ground. Anthes concluded that vegetation bands or patches on the order of 50–100 km wide in semi-arid regions could result

in greater increases in convective precipitation than occur in areas of uniform vegetation, owing to the development of (i) spatial variations in vertical wind velocities, and (ii) mesoscale (20–200 km) circulation systems. Pielke *et al.* (1991) demonstrated that mesoscale landscape spatial variability must be explicitly modelled in large-scale climate models. In Pielke *et al.* (1993), the authors showed that, on the Great Plains and in the Front Range of the Rocky Mountains, the spatial heterogeneity of land cover and vegetation type must be specified to properly calculate the fluxes of momentum and sensible and latent heat to the larger scale circulation of the atmosphere. In addition, they reported that the specific location and hour of the day that thunderstorms occur in their models depended on the spatial heterogeneity of the vegetation cover. These results are consistent with field and diagnostic studies by Garrett (1982), who found that the spatial heterogeneity of surface roughness, soil moisture, and forest coverage and transpiration affect the location and pace of convective cloud and rainfall formation.

To determine which attributes of the biosphere are important in model behaviour, a series of sensitivity tests have been performed on biosphere boundary conditions (Charney *et al.* 1977; Sud & Smith 1984; Cunnington & Rowntree 1986; Lavel & Picon 1986; Sud & Molod 1988; Lean & Warrilow 1989; Sato *et al.* 1989). These tests were designed to answer the following generic question: 'How large a climate change results from a specified change in a boundary condition of the biosphere?' Three general areas of sensitivity testing were conducted: biosphere surface roughness (Sud & Smith 1985a), biosphere evapotranspiration (Shukla & Mintz 1982), and biosphere albedo (Charney *et al.* 1977).

Studies by Chervin (1979), Sud & Fennessy (1984), Carson & Sangster (1982), and Mylne & Rowntree (1992) found the same results as Charney. On average they found a 20% decline in rainfall for each 0.1 increase in albedo. Rowntree (1983) also found that a 0.1 increase in albedo reduced evaporation by  $0.65 \text{ mm d}^{-1}$ . Garratt (1993) summarized the changes induced in evaporation and precipitation resulting from changes in model albedo. These changes are summarized below.

Albedos of most natural land-cover classes are not known through direct observation. Pielke & Avissar (1990) summarized published albedos for natural surfaces. In landscapes with mixed vegetation and exposed soils, albedos depend on soil albedos that are larger than vegetation, and may vary from 0.20 to 0.60. Clearly, the greatest potential for albedo change is in arid and semi-arid regions, and in areas subject to changes in cultural land use and variations in agricultural practices.

The homosphere is the lowest 30 km of the atmosphere where the chemical composition is relatively constant with altitude. The atmosphere above the homosphere is the heterosphere. In the heterosphere, photochemical processes dominate and chemical composition changes with increasing altitude. Numerous biogenic gases are emitted into the atmosphere that (i) play a fundamental role in the long-term equilibrium composition of the homosphere (Lovelock 1979), and (ii) play a role in the photochemistry of the heterosphere. Many gases added to the atmosphere by way of the biosphere ( $\text{H}_2\text{O}$ ,  $\text{O}_2$ ,  $\text{CO}_2$ ,  $\text{CO}$ ,  $\text{N}_2$ ,  $\text{N}_2\text{O}$ ,  $\text{NH}_4$ , and  $\text{CH}_4$ ) are well mixed in the

osphere (except H<sub>2</sub>O), and are radiatively active trace gases that contribute to the emissivity of the atmosphere and the planetary greenhouse. Greenhouse warming due to these trace gases is extensively reviewed elsewhere and will not be dealt with here. In addition, Lovelock (1979) emphasized their significance to 'planetary homeostasis' and this is the core of his Gaia hypothesis. Increasing concentrations of CO<sub>2</sub>, CH<sub>4</sub>, CFCs and N<sub>2</sub>O in the atmosphere at the core of the current prediction of global warming. Little is known about the long-term variation of total water vapour in the atmosphere. Cloudiness over continents has increased significantly during this century (Henderson-Sellers 1989). The causes of this increase are not known. Warming caused by other trace gases should increase atmospheric water vapour and further increase the warming by means of the emissivity of water vapour itself (Arrhenius 1896). Modern GCMs include this positive feedback, which accounts for a significant fraction of the warming seen in the output of these models.

The role of biogenic gases in heterospheric chemistry involves around H<sub>2</sub>O, CH<sub>4</sub>, O<sub>2</sub>, and methylated halogens. Anthropogenic chlorofluorocarbons have been implicated in photochemical losses of O<sub>3</sub> since 1969, but not by the increases in O<sub>3</sub> before 1969 (Ellsaesser 1982). Water vapour in the heterosphere is implicated in ozone depletion. Methane oxidation gives rise to hydroxyl radicals and ozone depletion in the upper atmosphere.

Biogenic non-methane hydrocarbons of continental origin are mixed throughout the troposphere, and are entrained in a layer at the boundary between the troposphere and the stratosphere: the tropopause. The attenuation of the solar beam by the particulate organic carbon in this layer amounts to about 1% of incoming solar radiation (Bodhaine & Pueschel 1974). Since the early part of the century, this attenuation of the solar beam has been found to have a distinct seasonal modulation, with an annual maximum in the summer (Flowers *et al.* 1969; Poeschel *et al.* 1972). Bodhaine & Pueschel (1974) attributed the summer solar radiation attenuation maximum observed at Auna Loa to the background biogenic hydrocarbons of continental origin. Chesselet *et al.* (1981) noted that particulate organic carbons in the marine atmosphere of less than 100 km have isotopic signatures typical of continental hydrocarbons. Went *et al.* (1967) sampled the filters from Trans World Airlines, and found vast quantities of jet black material, 90% of which was organic hydrocarbons, which were opaque in the infrared, like carbon black. These observations led to the conclusion that atmospheric loading by biogenic hydrocarbons directly attenuates incoming solar radiation and plays an important role in planetary energy budgets.

## DISCUSSION

I began this paper with Walter & Breckle's (1985) formulation of the long-standing paradigm about the role that the climate has on vegetation at all scales, from the microscale, limited control of vegetation on climate. Evidence for the shortcomings of this paradigm has been presented and an alternative explanation offered: at all scales, the climate controls the biosphere and the biosphere controls the climate. These are not the

only controls on either the biosphere or the climate. Rather, to understand the Earth's system dynamics and to successfully model and perhaps predict the future course of our environment, the linkages and controls are of such magnitude that they must be considered.

More specific lessons are:

1. Minimum and maximum temperatures are partially controlled by evapotranspiration and the emission of radiatively effective trace gases, including non-methane hydrocarbons.
2. Evapotranspiration contributes as much as half of precipitable water that falls on terrestrial ecosystems, which may be considered recycled rain.
3. Biogenic condensation and ice nuclei contribute to cloud formation and growth-cloud drop microphysics, and realized precipitation.
4. The atmosphere is a biogeochemical creation, the composition of which is maintained by a flux of important gases from the biosphere.
5. Gaseous emissions from the biosphere modulate both solar and terrestrial radiation budgets.
6. The spatial heterogeneity of ecosystems is responsible for some aspects of mesoscale patterns of the fluxes of mass, energy, and momentum from the biosphere to the atmosphere, and it modifies convective weather systems.
7. Sensitivity tests using GCMs indicate that large-scale climates are highly sensitive to evapotranspiration, vegetation albedo, and vegetation surface roughness.
8. Gaseous emissions from the biosphere are important reactants to the photochemical dynamics of the heterosphere.
9. The biosphere is an active agent in the control of climates at all scales and, if man is considered a member of the biosphere, anthropogenic controls on climate apply as well.

Support for the research in this contribution was provided by the National Science Foundation (grant no. DEB 92-11772). Support for the development of the manuscript was provided by the Sustainable Biosphere Initiative of Ecological Society of America through a grant from the Environmental Protection Agency (EPA). Steve Running, John Sigmon, and an anonymous reviewer at the EPA provided useful comments on this paper.

## REFERENCES

- Andreae, M. O. 1980 The production of methylated sulfur compounds by marine phytoplankton. In *Biogeochemistry of ancient and modern environments* (ed. P. A. Trudinger, M. R. Walter & B. J. Ralph), pp. 253–259. Berlin: Springer.
- Anthes, R. A. 1984 Enhancement of convective precipitation by mesoscale variations in vegetative covering in semiarid regions. *J. Clim. Appl. Met.* **23**, 540–553.
- Arrhenius, S. 1896 On the influence of carbonic acid in the air upon the temperature of the ground. *Phil. Mag. J. Sci.* **41** (251), 237–276.
- Avissar, R. 1992 Conceptual aspects of a statistical–dynamical approach to represent landscape subgrid-scale heterogeneities in atmospheric models. *J. Geophys. Res.* **97** (D3), 2729–2742.
- Becquerel, A. 1853 Connection between forest and climate. In *Forest influences*, 1st edn (ed. J. Kittredge), 394 pp. New York: McGraw-Hill.

- Bodhaine, B. A. & Pueschel, R. F. 1974 Source of seasonal variations in solar radiation at Mauna Loa. *J. Atmos. Sci.* **31**, 840–845.
- Borchert, J. R. 1950 The climate of the central North American grassland. *Ann. Assoc. Am. Geogr.* **60**(1), 1–39.
- Brubaker, K. L., Entekhabi, D. & Eagleson, P. S. 1993 Estimation of continental precipitation recycling. *J. Clim.* **6**, 1077–1089.
- Carson, D. J. & Sangster, A. B. 1981 The influence of land-surface albedo and soil moisture on GCM circulation. In *Numerical experimentation programme*, pp. 5.14–5.21. Report No. 2, UK Meteorology Office. Bracknell, England.
- Chang, F. & Wallace, J. M. 1987 Meteorological conditions during heat waves and droughts in the United States Great Plains. *Monthly Weather Rev.* **115**, 1253–1269.
- Charlson, R. J., Lovelock, J. E., Andreae, M. O. & Warren, S. F. 1987 Oceanic phytoplankton, atmospheric sulphur, cloud albedo and climate. *Nature* **326**, 655–661.
- Charney, J. G., Quirk, W. J., Chow, S. H. & Kornfield, J. 1977 A comparative study of the effects of albedo change on drought in semi-arid regions. *J. Atmos. Sci.* **34**, 1366–1385.
- Chervin, R. M. 1979 Response of the NCAR GCM to changed land surface albedo. *Report of the Joint Ocean Climate Change Study Conference on Climate Models: performance, intercomparison and sensitivity studies* **1**, 563–581.
- Chesselet, R., Fontugne, M., Buat-Menard, P., Ezat, U. & Lambert, C. E. 1981 The origin of particulate organic carbon in the marine atmosphere as indicated by its stable carbon isotopic composition. *Geophys. Res. Lett.* **8**(4), 345–348.
- Cunnington, W. M. & Rowntree, P. R. 1986 Simulations of the Saharan atmosphere—dependence on moisture and albedo. *Q. J. R. Met. Soc.* **112**, 971–999.
- Davies, C. N. 1974 Particulates in the atmosphere: natural and man-made. *Atmos. Environ.* **8**, 1069–1079.
- Dickinson, R. E., Henderson-Sellers, A., Kennedy, P. J. & Wilson, M. R. 1986 Biosphere atmosphere transfer scheme (BATS) for the NCAR community climate model. Technical note TN-275 + STR. Boulder, CO: National Center for Atmospheric Research.
- Duce, R. A., Quinn, G. & Wade, L. 1974 Residence time of non-methane hydrocarbons in the atmosphere. *Mar. Pollution Bull.* **5**, 59–61.
- Ellsaesser, H. W. 1982 Should we trust models or observations? *Atmos. Environ.* **16**(2), 197–205.
- Fennessy, M. M. (and 10 others) 1994 The simulated Indian monsoon: a GCM sensitivity study. *J. Clim.* **7**(1), 33–41.
- Flowers, E. C., McCormick, R. A. & Kurfis, K. R. 1969 Atmospheric turbidity over the United States, 1961–1966. *J. Appl. Met.* **8**, 955–962.
- Garratt, J. R. 1993 Sensitivity of climate simulations to land-surface and atmospheric boundary-layer treatments—a review. *J. Clim.* **6**, 419–449.
- Garrett, A. J. 1982 A parameter study of interactions between convective clouds, the convective boundary layer, and a forested surface. *Monthly Weather Rev.* **110**, 1041–1059.
- Hansen, J., Johnson, D., Lacs, A., Lebedeff, S., Lee, P., Rind, D. & Russell, G. 1981 Climate impact of increasing atmospheric carbon dioxide. *Science* **213**, 957–966.
- Henderson-Sellers, A. 1989 North American total cloud amount variation this century. *Global Planetary Change Section* **75**, 175–194.
- Hopp, R. J. 1974 Plant phenology observation networks. In *Phenology and seasonality modeling* (ed. H. Lieth), pp. 25–43. New York: Springer.
- Hough, F. B. 1877 Connection between forests and climate. In *Forest influences*, 1st edn (ed. J. Kittredge), 394 pp. New York: McGraw-Hill.
- Hudson, J. G. 1991 Observations of anthropogenic CCN. *Atmos. Environ.* **25A**(11), 2449–2455.
- Joussaume, S., Sadourny, R. & Vignal, A. 1986 Origin of precipitating water in a numerical simulation of the July climate. *Ocean–Air Interact.* **1**, 043–056.
- Junge, C. 1951 Nuclei of atmospheric condensation. In *Compendium of meteorology* (ed. T. F. Malone). Boston, MA: American Meteorological Society.
- Keen, B. 1959 *The life of the Admiral Christopher Columbus*. Brunswick, NJ: Rutgers University Press.
- Kittredge, J. 1948 *Forest influences*. New York: McGraw-Hill.
- Lander, G., Morgan, G., Nagamoto, C. T., Solak, M. & Rosinski, J. 1980 Generation of ice nuclei in the surface outflow of thunderstorms in Northeast Colorado. *J. Atmos. Sci.* **36**, 2484–2494.
- Lavel, K. & Picon, L. 1986 Effect of a change of the surface albedo of the Sahel on climate. *J. Atmos. Sci.* **43**, 2418–2429.
- Lean, J. & Warrilow, D. A. 1989 Simulation of the regional climatic impact of Amazon deforestation. *Nature* **342**, 411–413.
- Letteau, H., Letteau, K. & Molion, L. C. B. 1979 Amazonia's hydrologic cycle and the role of atmospheric recycling in assessing deforestation effects. *Monthly Weather Rev.* **107**(3), 227–238.
- Lovelock, J. E. 1979 *Gaia: a new look at life on Earth*. Oxford University Press.
- Manabe, S. & Wetherald, R. T. 1975 The effects of doubling the CO<sub>2</sub> concentration on the climate of a general circulation model. *J. Atmos. Sci.* **32**, 3–15.
- Moore, H. 1976 The organic constituents of atmospheric particulate matter. *Atmos. Environ.* **10**, 1037–1039.
- Mylne, M. F. & Rowntree, P. R. 1992 Modelling the effects of albedo change associated with tropical deforestation. *Clim. Change* **21**, 317–343.
- Nemani, R., Pierce, L., Running, S. & Band, L. 1993 Forest ecosystem processes at the watershed scale: sensitivity to remotely-sensed leaf area index estimates. *Int. J. Remote Sens.* **14**(13), 2519–2534.
- Nobre, C. A., Sellers, P. J. & Shukla, J. 1991 Amazonian deforestation and regional climate change. *J. Clim.* **4**, 957–988.
- Oort, A. H. 1964 On estimates of the atmospheric energy cycle. *Monthly Weather Rev.* **92**, 483–493.
- Peterson, J. T. & Junge, C. E. 1971 Sources of particulate matter in the atmosphere. In *Man's impact on the climate* (ed. W. H. Mathews), pp. 310–320. Cambridge, MA: MIT Press.
- Pielke, R. A. & Avissar, R. 1990 Influence of landscape structure on local and regional climate. *Landscape Ecol.* **4**, 133–155.
- Pielke R. A., Dalu, G. A., Snook, J. S., Lee, T. J. & Kittel, T. G. F. 1991 Nonlinear influence of mesoscale land use on weather and climate. *J. Clim.* **4**, 1053–1069.
- Pielke, R. A., Schimel, D. S., Lee, T. J., Kittel, T. G. F. & Zeng, X. 1993 Atmosphere–terrestrial ecosystem interactions: implications for coupled modelling. *Ecol. Model.* **67**, 5–18.
- Pkhalagov, Y. A., Uzhegov, V. N. & Shchelkanov, N. N. 1987 Some optical characteristics of the spring atmosphere of desert areas. *Izvestiya Atmos. Ocean. Phys.* **23**(4), 306–310.
- Priestley, C. H. B. & Taylor, R. J. 1972 On the assessment of surface heat flux and evaporation using large-scale parameters. *Monthly Weather Rev.* **100**(2), 81–92.
- Pueschel, R. F., Ellis, H. T., Cotton, G. F., Flowers, E. C. & Peterson, J. T. 1972 Normal incidence solar radiation trends on Mauna Loa, Hawaii. *Nature* **240**, 545–547.
- Rasmussen, R. A. 1972 What do hydrocarbons from trees contribute to air pollution? *J. Air Pollution Control Assoc.* **22**(7), 537–543.
- Rasmussen, R. A. & Went, F. W. 1965 Volatile organic matter of plant origin in the atmosphere. *Proc. Natn. Acad. Sci. USA* **53**, 215–220.
- Rasmusson, E. M. 1967 Atmospheric water vapor transport and the water balance of North America. I. Characteristics of the water vapor flux field. *Monthly Weather Rev.* **95**(7), 403–426.

- ousson, E. M. 1968 Atmospheric water vapor transport and water balance of North America. II. Large-scale water balance investigations. *Monthly Weather Rev.* **96**(10), 720–734.
- ousson, E. M. 1971 A study of the hydrology of eastern North America using atmospheric vapor flux data. *Monthly Weather Rev.* **99**(2), 120–135.
- ousson, G. D. 1950 Notes measurement and estimation of atmospheric radiation. *Q. J. R. Met. Soc.* **76**, 37–51.
- ousson, G. D. 1968 Some determinations of atmospheric absorption by measurement of solar radiation from aircraft and at the surface. *Q. J. R. Met. Soc.* **92**, 215.
- ousson, E. & Robbins, R. C. 1970 Gaseous nitrogen compound pollutants from urban and natural sources. *J. Air Pollution Control Assoc.* **22**(7), 537–543.
- ouza, R. D. & Omolayo, A. S. 1981 Exchange of water vapor between land and ocean in the Northern Hemisphere. *J. Geophys. Res.* **86**(C12), 147, 152.
- outree, P. R. 1983 Simulation of atmospheric response to soil moisture anomalies over Europe. *Q. J. R. Met. Soc.* **109**, 501–513.
- oung, S. W., Nemani, R. R. & Hungerford, R. D. 1987 Interpolation of synoptic meteorological data in mountainous terrain and its use for simulating forest evapotranspiration and photosynthesis. *Can. J. Forest Res.* **17**, 472–483.
- oung, S. W., Loveland, T. R. & Pierce, L. L. 1994 A vegetation classification logic based on remote sensing for use in global biogeochemical models. *Ambio* **23**(1), 77–81.
- ouli, E., Dall'Oliio, A., Matsui, E. & Gat, J. R. 1979 Recycling of water in the Amazon Basin: an isotopic study. *Water Resources Res.* **15**(5), 1250–1258.
- oulin, N., Sellers, P. J., Randall, D. A., Schneider, E. K., Shukla, K., Kinter, J. L. III, Hou, Y.-T. & Albertazzi, E. 1989 Effects of implementing the simple biosphere model in a general circulation model. *J. Atmos. Sci.* **46**(18), 2757–2782.
- ouler, V. J. 1970 Condensation nuclei: production of very large numbers in country air. *Science* **170**, 851–852.
- oull, R. C. 1975 Ice nuclei produced by laboratory cultured marine phytoplankton. *Geophys. Res. Lett.* **2**(11), 500–503.
- oull, R. C. & Vali, G. 1972 Atmospheric ice nuclei from decomposing vegetation. *Nature* **236**, 163–165.
- oull, R. C. & Vali, G. 1973 World-wide source of leaf-derived freezing nuclei. *Nature* **246**, 212–213.
- oull, R. C. & Vali, G. 1976 Biogenic ice nuclei. I. Terrestrial and marine sources. *J. Atmos. Sci.* **33**, 1554–1564.
- oull, R. C., Worbel, B. & Miller, S. W. 1980 Seasonal changes and terrestrial sources of atmospheric ice nuclei at Boulder, Colorado. *AIMPA Commission Int. de Physique des Neiges* **1**, 42–46.
- ouler, S. H. 1992 *Global warming*. San Francisco, CA: Sierra Club Books.
- ouler, S. H. & Mesirov, L. E. 1976 *The genesis strategy: climate and global survival*. New York: Plenum Press.
- ouler, S. E. 1988 Are global cloud albedo and climate controlled by marine phytoplankton? *Nature* **336**, 441–445.
- ouler, M. D. 1992 Phenology and springtime surface layer change. *Monthly Weather Rev.* **120**, 2570–2578.
- ouler, M. D. 1998 Monitoring global change with phenology: the case of the spring green wave. *Int. J. Biometeorol.* (In the Press.)
- Schwartz, M. D. & Karl, T. R. 1990 Spring phenology: nature's experiment to detect the effect of 'green-up' on surface maximum temperatures. *Monthly Weather Rev.* **118**, 883–890.
- Sellers, W. D. & Dryden, P. S. 1967 *An investigation of heat transfer from bare soil. Final report: grant DA-AMC-28-043-66-627*. Tucson, AZ: Institute of Atmospheric Physics, University of Arizona.
- Sellers, P. J., Mintz, Y., Sud, Y. C. & Dalcher, A. 1986 A simple biosphere model (SiB) for use within general circulation models. *J. Atmos. Sci.* **43**, 505–531.
- Shukla, J. & Mintz, Y. 1982 Influence of land-surface evapotranspiration on the Earth's climate. *Science* **215**, 1498–1501.
- Staley, D. O. & Jurica, G. M. 1970 Flux emissivity tables for water vapor, carbon dioxide and ozone. *J. Appl. Met.* **9**, 365–372.
- Staley, D. O. & Jurica, G. M. 1971 Effective atmospheric emissivity under clear skies. *J. Appl. Met.* **11**, 349–356.
- Stephens, E. R. & Price, M. A. 1970 Smog aerosol: infrared spectra. *Science* **168**, 1584–1586.
- Sud, Y. C. & Fennessy, M. J. 1984 Influence of evaporation in semi-arid regions on the July circulation: a numerical study. *Boundary Layer Met.* **33**, 185–210.
- Sud, Y. C. & Molod, A. 1988 A GCM simulation study of the influence of Saharan evapotranspiration and surface-albedo anomalies on July circulation and rainfall. *Monthly Weather Rev.* **116**, 2388–2400.
- Sud, Y. C. & Smith, W. E. 1984 Ensemble formulation of surface fluxes and improvement in evapotranspiration and cloud parameterization in a GCM. *Boundary Layer Met.* **29**, 185–210.
- Sud, Y. C. & Smith, W. E. 1985a The influence of surface roughness of deserts on the July circulation. *Boundary Layer Met.* **33**, 15–49.
- Sud, Y. C. & Smith, W. E. 1985b Influence of local land-surface processes on the Indian monsoon: a numerical study. *J. Clim. Appl. Met.* **24**, 1015–1036.
- Tyndall, J. 1865 *Heat: a mode of motion*. New York: D. Appleton and Co.
- Vali, G., Christiansen, M., Fresh, R. W., Galyan, E. L., Make, L. R. & Schnell, R. C. Biogenic ice nuclei. II. Bacterial sources. *J. Atmos. Sci.* **33**, 1565–1570.
- Walter, H. & Breckle, S. 1985 *Ecological systems of the geobiosphere*. Berlin: Springer.
- Went, F. W. 1960 Blue hazes in the atmosphere. *Nature* **187**, 641–643.
- Went, F. W. 1964 The nature of Aitken condensation nuclei in the atmosphere. *Proc. Natn. Acad. Sci. USA* **51**, 1259–1267.
- Went, F. W. 1966 On the nature of Aitken condensation nuclei in the atmosphere. *Tellus* **18**(2), 549–556.
- Went, F. W., Simmons, D. B. & Monzingo, H. N. 1967 The organic nature of atmospheric condensation nuclei. *Proc. Natn. Acad. Sci. USA* **58**, 69–74.
- Wigley, T. M. L. 1989 Possible climate change due to SO<sub>2</sub>-derived CCN. *Nature* **339**, 365–367.
- Williams, M. D., Treiman, E. & Wecksung, M. 1980 Plume blight visibility modeling with a simulated photograph technique. *J. Air Pollution Control Assoc.* **30**(2), 12 130.
- Woodcock, A. H. & Gifford, M. M. 1949 Sampling atmospheric sea-salt nuclei over the oceans. *J. Mar. Res.* **8**, 177–197.